Neuro-Oncology
22(2), 240–252, 2020 | doi:10.1093/neuonc/noz183 | Advance Access date 24 September 2019

TSPO deficiency induces mitochondrial dysfunction, leading to hypoxia, angiogenesis, and a growth-promoting metabolic shift toward glycolysis in glioblastoma

Yi Fu,[#] Dongdong Wang,[#] Huaishan Wang, Menghua Cai, Chao Li, Xue Zhang, Hui Chen, Yu Hu, Xuan Zhang, Mingyao Ying, Wei He, and Jianmin Zhang

Department of Immunology, Research Center on Pediatric Development and Diseases, Institute of Basic Medical Sciences, Chinese Academy of Medical Sciences and School of Basic Medicine, Peking Union Medical College, State Key Laboratory of Medical Molecular Biology, Beijing, China (Y.F., D.W., H.W., M.C., C.L., X.Z., H.C., Y.H., W.H., J.Z.); Department of Rheumatology and Clinical Immunology, Peking Union Medical College Hospital, Chinese Academy of Medical Sciences and Peking Union Medical College, Beijing, China (X.Z.); Hugo W. Moser Research Institute at Kennedy Krieger, and Department of Neurology, Johns Hopkins School of Medicine, Baltimore, Maryland, USA (M.Y.)

Corresponding Authors: Jianmin Zhang, Ph.D. Department of Immunology, Research Center on Pediatric Development and Diseases, Institute of Basic Medical Sciences, Chinese Academy of Medical Sciences and School of Basic Medicine, Peking Union Medical College, State Key Laboratory of Medical Molecular Biology, Beijing, 100005, China (jzhang@ibms.pumc.edu.cn); Wei He, M.D., (heweingd@126.com).

[#]These authors contributed equally to this work.

Abstract

Background. The ligands of mitochondrial translocator protein (TSPO) have been widely used as diagnostic biomarkers for glioma. However, the true biological actions of TSPO in vivo and its role in glioma tumorigenesis remain elusive.

Methods. TSPO knockout xenograft and spontaneous mouse glioma models were employed to assess the roles of TSPO in the pathogenesis of glioma. A Seahorse Extracellular Flux Analyzer was used to evaluate mitochondrial oxidative phosphorylation and glycolysis in TSPO knockout and wild-type glioma cells.

Results. TSPO deficiency promoted glioma cell proliferation in vitro in mouse GL261 cells and patient-derived stem cell–like GBM1B cells. TSPO knockout increased glioma growth and angiogenesis in intracranial xenografts and a mouse spontaneous glioma model. Loss of TSPO resulted in a greater number of fragmented mitochondria, increased glucose uptake and lactic acid conversion, decreased oxidative phosphorylation, and increased glycolysis.

Conclusion. TSPO serves as a key regulator of glioma growth and malignancy by controlling the metabolic balance between mitochondrial oxidative phosphorylation and glycolysis.

Key Points

1. TSPO deficiency promotes glioma growth and angiogenesis.
2. TSPO regulates the balance between mitochondrial oxidative phosphorylation and glycolysis.

© The Author(s) 2019. Published by Oxford University Press on behalf of the Society for Neuro-Oncology. All rights reserved.
For permissions, please e-mail: journals.permissions@oup.com

Importance of the Study

This study uncovers a novel function of TSPO in the regulation of glioma growth and angiogenesis by controlling the metabolic balance between oxidative phosphorylation and glycolysis. Our findings provide new insights into the biological actions of TSPO in regulating mitochondrial function, cellular metabolism, and tumorigenesis.

The mitochondrial translocator protein (TSPO), previously known as the peripheral benzodiazepine receptor, is an evolutionarily conserved 18 kDa transmembrane protein primarily located in the outer mitochondrial membrane.[1] TSPO was originally believed to function in mediating mitochondrial cholesterol import for steroid hormone production, which is essential for many physiological processes.[2] However, the results of recent studies, including our previous study examining in vivo and in vitro genetic *Tspo*-deficient models, have strongly refuted the previously proposed function of TSPO in regulating cholesterol transport and steroid biosynthesis.[3,4] TSPO-knockout (KO) mice exhibited normal viability, fertility, and the ability to generate steroid hormones.[3,4] A fundamental gap exists in our understanding of the function of TSPO in association with various cellular processes and diseases, including cell proliferation, inflammatory responses, and tumor progression.[5,6] Therefore, further experiments are necessary to determine the functions of TSPO in physiological and pathological conditions.

TSPO expression is believed to be highly upregulated in many inflammatory diseases and various tumor types, such as glioma.[6–8] This notable phenomenon provides an important clue regarding the physiological function of TSPO. Glioblastoma (GBM) is the most common and malignant type of glioma, accounting for 60–70% of all primary brain tumor diagnoses in adults.[9] TSPO is highly expressed in human gliomas,[8] which has sparked investigations into TSPO as a diagnostic biomarker for glioma.[10] Several clinical trials using PET with radiolabeled TSPO ligands, such as ^{11}C-PK11195, have shown specific tumor uptake and a good capacity to monitor and quantify tumor progression.[11] However, the role of TSPO in glioma remains controversial, and the underlying molecular mechanisms are unknown.

In this study, we characterized the roles of TSPO in glioma pathogenesis using in vivo TSPO-KO mouse models and in vitro CRISPR/Cas9-based TSPO-deficient glioma cell models. TSPO deficiency promotes glioma proliferation and angiogenesis and serves as a key regulator of the dynamic balance between oxidative phosphorylation and glycolysis. Our findings provide novel insights into the biological actions of TSPO under physiological and pathological conditions and a better understanding of the molecular events responsible for glucose metabolism.

Materials and Methods

The Animal Care and Use Committee at the Institute of Basic Medical Sciences, Chinese Academy of Medical Sciences, approved this project. The reagents, cells, and mice used in this study are described in the Supplementary Material.

Detection of TSPO Expression on GBM Tissue Array

A human GBM tissue microarray was purchased from US Biomax. Immunohistochemical staining for TSPO was performed using an anti-TSPO antibody as described in the Supplementary Material.

Generation of TSPO-Knockout GL261 Cells with the CRISPR/Cas9 System

TSPO-KO GL261 cells were generated using the CRISPR/Cas9 system targeting the mouse *TSPO* exon 2 region to ensure an effective single-guide RNA, as described in the Supplementary Material.

Intracranial Xenograft Glioma Mouse Model

TSPO-KO GL261 cells and wild-type (WT) GL261 cells were suspended in Dulbecco's modified Eagle's medium at 1.0×10^5 cells in 5 μL of medium before being intracranially injected into the brains of TSPO-KO mice or WT littermates as described previously.[12] See the Supplementary Material for more details.

Mitochondrial Morphology Imaging

MitoTracker Red CMXRos (Invitrogen) was applied to label the mitochondria of GL261 cells as described previously.[13] See the Supplementary Material for more details.

Mitochondrial Stress Test Assay and Glycolysis Stress Test Assay

XF Cell Mito Stress Test Kits and the XF Glycolysis Stress Test Kit were employed to measure mitochondrial function and glycolytic function using an Extracellular Flux Analyzer (Seahorse Bioscience) as described previously.[14] See the Supplementary Material for more details.

Data Analysis

Unpaired two-tailed Student's *t*-test was performed to analyze the statistical significance of two-group comparisons.

The comparison of more than two groups was analyzed by ANOVA with Bonferroni's post hoc test. The Gehan-Breslow-Wilcoxon test was used to calculate the significance of the survival curves. The data are presented as mean ± standard deviation, except where otherwise indicated. $P \leq 0.05$ was considered significant.

Results

TSPO Is Highly Expressed in Human Glioma

We performed immunohistochemical analyses using human grade IV glioma (GBM) tissue arrays with 35 duplicate GBM tissues and 5 duplicate normal brain tissues to examine TSPO expression in human GBM. The TSPO protein was expressed at approximately 3.5-fold higher levels in GBM tissues than in normal brain tissues (Supplementary Figure 1A and B). We also analyzed The Cancer Genome Atlas glioma databases and obtained similar results. Significantly higher levels of TSPO mRNA were also observed in glioma specimens than in normal brain tissues (Supplementary Figure 1C). These findings demonstrated that TSPO expression is upregulated in GBM tissues. Previous studies reported that TSPO expression in human astrocytomas was correlated with the grade of malignancy and survival.[8,15] Thus, we analyzed the survival rates of patients with human GBM from The Cancer Genome Atlas database. However, we did not observe a significant correlation of TSPO expression with the survival rates of patients with GBM (Supplementary Figure 1D–G). In contrast, patients with neural GBM who presented low levels of the TSPO protein exhibited slightly shorter survival times than patients with high levels of TSPO expression (Supplementary Figure 1H). In addition, we examined the expression levels of the angiogenesis regulator vascular endothelial growth factor A (VEGF-A) and the glycolysis associated enzyme **lactate dehydrogenase A (**LDHA) on GBM tissue arrays. The results showed that the average levels of TSPO, VEGF-A, and LDHA in GBM tissues were higher than those in normal brain tissues, but they were very heterogeneous (Supplementary Figure 2A). No significant correlation between TSPO expression with the level of VEGF-A or LDHA in GBM was observed (Supplementary Figure 2B and C). While some GBM tissues showed high expression levels of all these proteins, many GBM samples with low TSPO expression displayed high levels of VEGF-A and LDHA, and multiple samples with high TSPO expression exhibited relatively low levels of VEGFA and LDHA (Supplementary Figure 2A–C). These results indicated that elevated TSPO expression in human GBM tissues is not a common feature and not closely correlated with malignancy and patient survival. Therefore, the role of TSPO in glioma needs to be further investigated.

TSPO Deficiency Promotes the Proliferation of Glioma Cells

To study the role of TSPO in glioma, we established a TSPO-deficient cell model using the CRISPR/Cas9 system in mouse GL261 glioma cells. We designed 3 single-guide RNAs of TSPO targeting exon 2 (Supplementary Figure 3A). Two GL261 lines with a 2-bp (clone 1) or 5-bp (clone 2) shift mutation were established (referred to as TSPO-KO cells), and western blotting verified the complete loss of TSPO expression in TSPO-KO cells (Fig. 1A). Surprisingly, TSPO-KO cells displayed a higher proliferation rate than WT cells (Fig. 1B and C). In the Cell Counting Kit 8 (CCK-8) cell proliferation assay, both TSPO-KO clones exhibited an approximately 30% increase in proliferation at 48 hours compared with the 2 WT clones (Fig. 1C). The viability of TSPO-KO cells was also found to increase (Supplementary Figure 3B). However, the proliferative activity of mouse embryonic fibroblasts (MEFs) from TSPO-KO mice showed no change compared with WT MEFs from WT littermates (Supplementary Figure 3C). Taken together, these results suggest that the loss of TSPO enhances GL261 cell proliferation but does not affect normal somatic cells in TSPO KO mice.

Cell cycle progression is a key regulator of cell proliferation; thus, we examined whether TSPO deletion affected the cell cycle progression of GL261 cells. More TSPO-KO cells were found in S phase than in G0/1 phase (Fig. 1D and E), indicating that the TSPO deletion affected cell cycle progression, which may contribute to the increased proliferation of TSPO-KO GL261 cells. Intriguingly, the apoptotic rate of TSPO-KO GL261 cells was increased as measured by caspase-3 activity (Supplementary Figure 3D).

TSPO Deficiency Promotes Glioma Growth and Malignancy in a Mouse GL261 Xenograft Glioma Model

To further determine whether TSPO deficiency promotes glioma growth and malignancy in vivo, TSPO-KO cells and WT GL261 cells were injected into the corpus striatum region of the brains of WT mice and TSPO-KO mice as described previously.[12] As shown in the survival curves, both WT and TSPO-KO mice bearing TSPO-KO GL261 cells died significantly earlier than mice bearing WT GL261 cells (Fig. 1F and Supplementary Figure 3E), indicating that TSPO deletion in glioma cells increased the tumor burden. Serial sections of brain tissues from tumor-bearing mice showed a significantly greater average volume of TSPO-KO gliomas than WT gliomas (Fig. 1G–I). Surprisingly, TSPO-KO gliomas exhibited extensive hemorrhagic areas (Fig. 1G and H), a common feature of highly malignant gliomas. Hematoxylin and eosin (HE) staining also indicated robust hemorrhaging and more abundant blood vessels in TSPO-KO tumors than in WT tumors (Fig. 1G and H). Taken together, these results suggest that the loss of TSPO promotes glioma growth and malignancy.

TSPO Deficiency Promotes Primary Glioma Pathogenesis in a Spontaneous Murine Glioma Model

Next, we sought to explore the effects of TSPO deficiency on the primary formation of glioma in a spontaneous glioma model using *S100b-v-ErbB*$^{+}$*Cdkn2a*$^{-/-}$ mice.[16] These mice were crossbred with TSPO-KO mice to generate

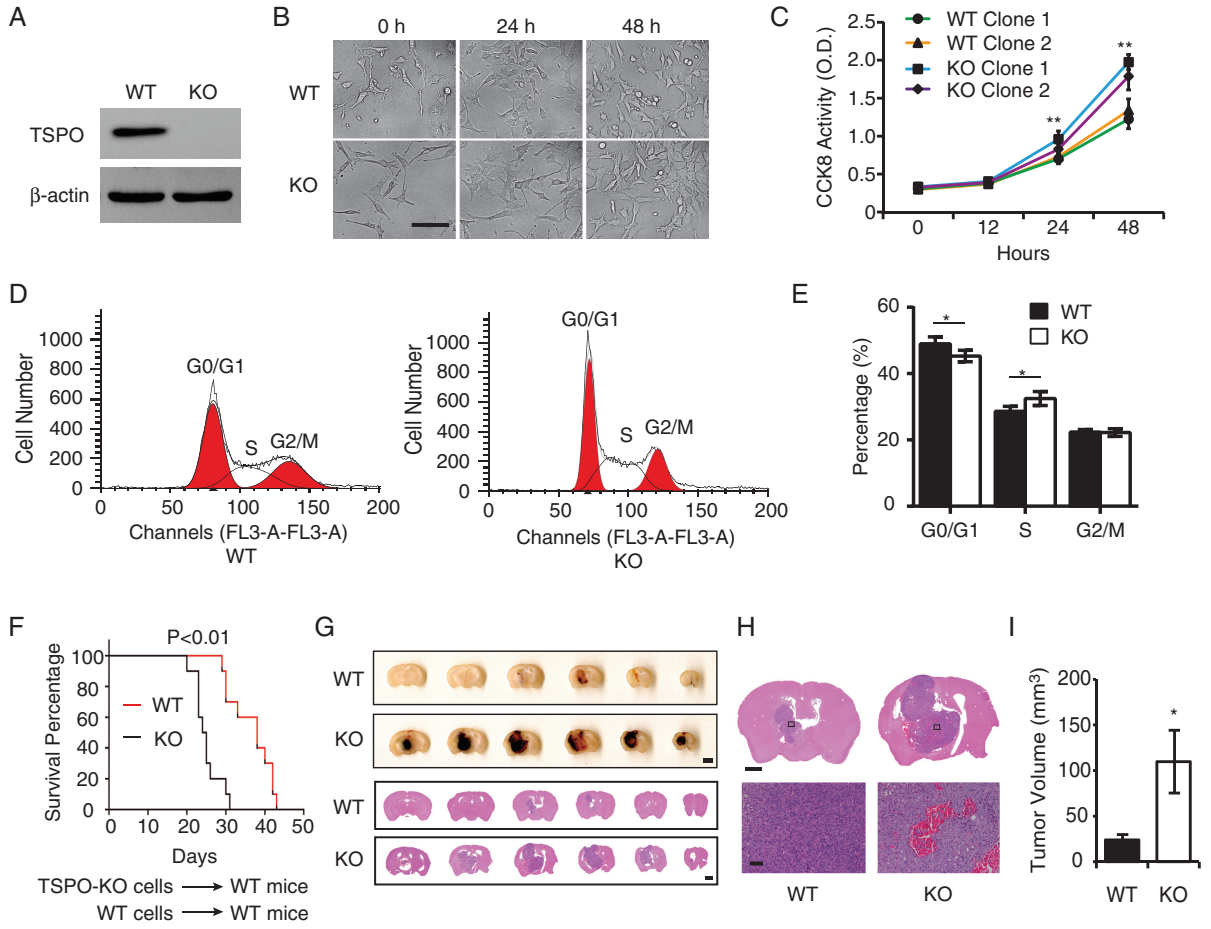

Fig. 1 TSPO deletion promotes the proliferation of glioma cells and the growth of glioma in an intracranial xenograft glioma model. (A) Western blot verified the loss of TSPO expression in TSPO-KO GL261 cells in which the gene was knocked out using the CRISPR/Cas9 system. (B) Images of TSPO-KO and WT GL261 cells were acquired at 0, 24, and 48 hours of culture. Scale bar, 100 μm. (C) CCK-8 assay. (D) Flow cytometry for cell cycle analysis. (E) Quantitation of the percentages of cells in different phases of the cell cycle shown in (D). (F) Survival curves for the mouse intracranial xenograft glioma model following the injection of WT or KO GL261 cells into the brains of WT mice. (G) Representative images of a series of slices from one mouse brain with glioma without staining (upper panel) or with HE staining (lower panel) captured 20 days after the intracranial injection of KO or WT cells. Scale bar, 1 mm for upper images and 100 μm for lower images. (H and I) High-resolution images of HE-stained brain slices (H) and the quantification of tumor volumes (I). Scale bar, 100 μm. Three independent experiments were performed. The data are presented as means ± SEM. $*P < 0.05$ and $**P < 0.01$ as determined using Student's *t*-test (C, E, and I) and the Gehan-Breslow-Wilcoxon test (F).

S100b-v-ErbB^{+}*Cdkn2a*$^{-/-}$*TSPO*$^{-/-}$ mice. In the survival analysis, *S100b-v-ErbB*$^{+}$*Cdkn2a*$^{-/-}$*TSPO*$^{-/-}$ mice died significantly earlier than their *S100b-v-ErbB*$^{+}$*Cdkn2a*$^{-/-}$*TSPO*$^{+/+}$ littermates (Fig. 2A), consistent with our findings from the TSPO-KO GL261 xenografts. An MRI analysis of T2-weighted scans confirmed that the majority of the *S100b-v-ErbB*$^{+}$*Cdkn2a*$^{-/-}$*TSPO*$^{-/-}$ mice died from severe solid gliomas, and some possibly died due to serious cerebral edema. The gliomas in *S100b-v-ErbB*$^{+}$*Cdkn2a*$^{-/-}$*TSPO*$^{-/-}$ mice were generated earlier and grew faster than those in *S100b-v-ErbB*$^{+}$*Cdkn2a*$^{-/-}$*TSPO*$^{+/+}$ controls (Fig. 2B). Extensive hemorrhagic areas were observed in all gliomas in *S100b-v-ErbB*$^{+}$*Cdkn2a*$^{-/-}$*TSPO*$^{-/-}$ mice (Fig. 2C and D). In summary, the 2 glioma models produced consistent results, indicating that TSPO deficiency promotes glioma growth and malignancy.

TSPO Deficiency Promotes Glioma Angiogenesis

The findings demonstrating that TSPO-KO gliomas exhibited extensive hemorrhaging led us to determine whether TSPO regulates angiogenesis in glioma. We stained WT and TSPO-KO glioma tissues for the angiogenesis marker CD31 (Fig. 2E and F) and performed western blotting (Fig. 2G and H). Consistently, more abundant CD31+ blood vessels were observed in TSPO-KO gliomas than in WT tumors (Fig. 2E–H). Then, we examined the levels of several angiogenesis regulators. VEGF-A, interleukin (IL)-8, and matrix metalloproteinase 2 (MMP2) levels were significantly increased in TSPO-KO gliomas compared with WT tumors, whereas no significant changes were observed in VEGF-C and MMP9 expression (Fig. 2G and H). Thus, TSPO appears to function as a key regulator of glioma angiogenesis.

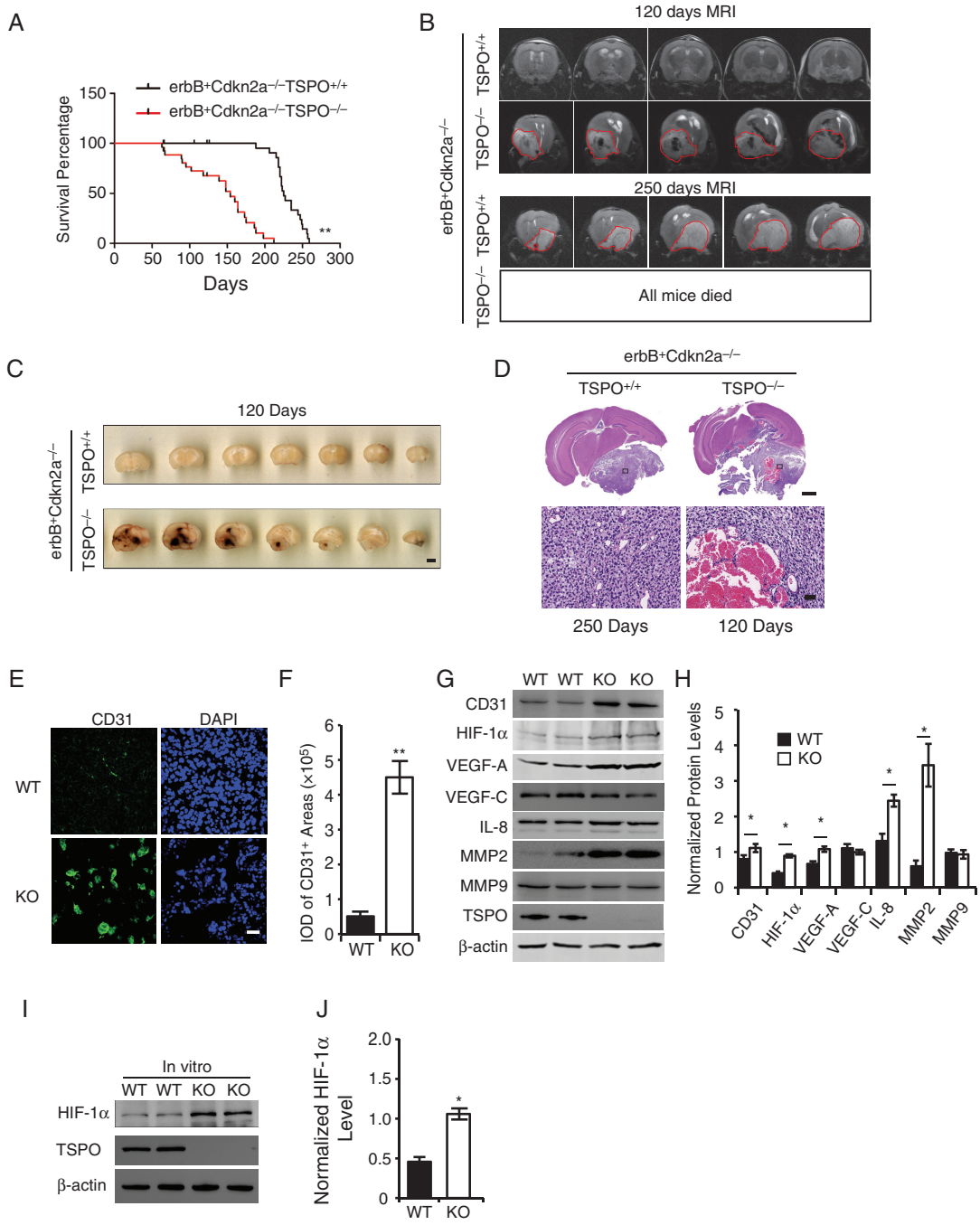

Fig. 2 TSPO deletion promotes glioma pathogenesis and malignancy in a spontaneous primary glioma mouse model by increasing hypoxia-induced angiogenesis. (A) Survival curves for *S100b-v-ErbB*$^{+}$*Cdkn2a*$^{-/-}$*TSPO*$^{-/-}$ mice (n = 27) and *S100b-v-ErbB*$^{+}$*Cdkn2a*$^{-/-}$*TSPO*$^{+/+}$ littermates (n = 26). (B) The upper panel shows representative MRIs of the brains of *S100b-v-ErbB*$^{+}$*Cdkn2a*$^{-/-}$*TSPO*$^{-/-}$ mice and *S100b-v-ErbB*$^{+}$*Cdkn2a*$^{-/-}$*TSPO*$^{+/+}$ littermates at the age of 120 days. The circled regions indicate the gliomas, which appear dark, suggesting extensive hemorrhaging in the gliomas. The lower panel shows a representative brain MRI of an *S100b-v-ErbB*$^{+}$*Cdkn2a*$^{-/-}$*TSPO*$^{+/+}$ mouse at the age of 250 days. The circled regions indicate the gliomas, which appear relatively white, suggesting little hemorrhaging. No brain MRIs were obtained from *S100b-v-ErbB*$^{+}$*Cdkn2a*$^{-/-}$*TSPO*$^{-/-}$ mice because all of these mice died before 210 days. (C) Representative images of a series of slices from *S100b-v-ErbB*$^{+}$*Cdkn2a*$^{-/-}$*TSPO*$^{-/-}$ mice and *S100b-v-ErbB*$^{+}$*Cdkn2a*$^{-/-}$*TSPO*$^{+/+}$ littermates at the age of 120 days. Scale bar, 2 mm. (D) Representative images of HE-stained brain slices from *S100b-v-ErbB*$^{+}$*Cdkn2a*$^{-/-}$*TSPO*$^{-/-}$ mice (120 days) and *S100b-v-ErbB*$^{+}$*Cdkn2a*$^{-/-}$*TSPO*$^{+/+}$ littermates (250 days). Scale bar, 1 mm for upper images and 100 μm for lower images. (E) Representative images of CD31 immunofluorescence staining of glioma tissues. Scale bar, 20 μm. (F) Quantification of CD31 levels in glioma tissues. (G) Western blot analysis of the levels of the angiogenesis-associated proteins in glioma tissues. (H) Quantification of the relative levels of angiogenesis-associated proteins shown in panel G compared with β-actin. (I) Western blot analysis of HIF-1α levels in TSPO-KO cells compared with WT cells. (J) Normalized HIF-1α levels in panel I. Three independent experiments were performed. The data are presented as means ± SEM. *P < 0.05 and **P < 0.01 as determined using Student's t-test (F, H, and J) or the Gehan-Breslow-Wilcoxon test (A).

Hypoxia enhances the malignant phenotypes of many solid tumors by activating hypoxia signaling pathways, such as hypoxia-inducible factors (HIFs), which play critical roles in promoting angiogenesis.[17] Thus, we measured HIF-1α levels in TSPO-KO GL261 cells and xenograft tumors using western blotting. Significantly higher HIF-1α levels were observed in TSPO-KO cell cultures and tumors than in WT controls (Fig. 2G–J). Based on these results, TSPO deficiency triggers HIF-1α upregulation and subsequently increases the levels of VEGF-A, IL-8, and MMP2, resulting in increased angiogenesis.

TSPO Deficiency Increases Mitochondrial Fragmentation in Glioma Cells

TSPO is an outer mitochondrial membrane protein. Consistently, we found good co-localization of TSPO with the MitoTracker signal in GL261 cells (Fig. 3A, upper panels). We thus examined whether TSPO loss affects mitochondrial morphology and function. We observed an obvious morphological change in the mitochondria in TSPO-KO GL261 cells stained with MitoTracker (Fig. 3A, lower panels). While WT GL261 cells contained more fused or elongated mitochondria, TSPO-deficient cells contained more round or fragmented mitochondria (Fig. 3A and B). The mitochondrial defects in TSPO-KO GL261 cells could be rescued by restoring the expression of TSPO fused with green fluorescent protein (GFP) but not by GFP alone (Fig. 3C and D), indicating that mitochondria fragmentation in TSPO-KO cells results specifically from TSPO deficiency. However, TSPO overexpression in WT GL261 cells did not induce obvious changes in mitochondrial morphology (Fig. 3C and D).

Next, we sought to determine whether TSPO deletion affected the levels of proteins related to mitochondrial fusion/fission. Western blots showed a significant increase in the levels of the mitochondrial fission proteins MFF (mitochondrial fission factor) and FIS1 (fission 1 protein) and a dramatic reduction in the level of the mitochondrial fusion protein Mfn-1 (mitofusin 1) in cells lacking TSPO (Fig. 3E and F). The levels of Mfn-2 and OPA1 (optic atrophy 1) were slightly increased, while levels of DRP1 (dynamin-related protein 1) were not noticeably altered. Levels of AMPKα (AMP-activated protein kinase alpha) were also increased in TSPO-KO cells, whereas the levels of complex I were decreased (Fig. 3E and F), suggesting a fundamental stress and energy deficiency in TSPO-KO cells.

TSPO Deficiency Decreases Mitochondrial Oxidative Phosphorylation Capacity and Increases Production of Reactive Oxygen Species in Glioma Cells

Fragmented mitochondria cause the dysfunction of mitochondrial metabolism.[18] We therefore assessed mitochondrial membrane potentials (MMPs) in live TSPO-KO cells and WT cells by staining for a membrane potential probe, tetramethylrhodamine methyl ester (TMRM), a cationic fluorescent dye that accumulates inside the mitochondrial matrix according to the MMPs. TSPO-KO GL261 cells were found to exhibit significantly lower MMPs than WT cells (Fig. 3G and H). In addition, we observed a significant decrease in global ATP production in TSPO-KO GL261 cells (Fig. 3I). Thus, TSPO deletion may impair mitochondrial respiratory function.

Next, we assessed mitochondrial function in TSPO-KO cells using a Seahorse Extracellular Flux XF24 Analyzer. As observed in the oxygen consumption rate curves, both the basal and maximal mitochondrial respiratory capacities were significantly decreased in TSPO-KO cells compared with WT cells (Fig. 3J and K). ATP production was also significantly reduced in TSPO-KO cells (Fig. 3J and K). In contrast, no significant changes in nonmitochondrial respiration were observed between TSPO-KO and WT cells (Fig. 3K). TSPO expression was restored by transfecting TSPO-GFP expression constructs into TSPO-KO cells. TSPO-GFP, but not GFP expression alone, rescued the impaired mitochondrial energy metabolism and oxidative phosphorylation capacity of TSPO-KO cells (Supplementary Figure 4A and B). Based on these results, TSPO deletion impairs mitochondrial energy metabolism and oxidative phosphorylation in glioma cells. In addition, we further evaluated the effect of TSPO deficiency on reactive oxygen species (ROS) production by performing live imaging of neurons incubated with H2DCFDA (2′,7′-dichlorodihydrofluorescein diacetate).[19] TSPO-KO GL261 cells displayed significantly higher ROS levels than WT cells (Fig. 3L and M), revealing a more hypoxic microenvironment in TSPO-KO GL261 cells.

TSPO Regulates the Glycolytic Capacity of GL261 Cells and Xenografts

Rather than generating energy via mitochondrial oxidative phosphorylation, tumor cells predominantly generate energy by initiating a high rate of glycolysis, followed by lactic acid fermentation in the cytosol, which is known as the "Warburg effect."[20] Thus, we sought to further examine whether TSPO deficiency affected glycolysis in GL261 cells using the Seahorse Extracellular Flux XF24 Analyzer, and we observed enhanced glycolysis in TSPO-KO cells (Fig. 4A and B). The rate of glycolysis, glycolytic capacity, and glycolytic reserve were significantly increased in TSPO-KO cells compared with WT cells. In contrast, no significant changes were observed for nonglycolytic acidification between WT and KO cells (Fig. 4A and B). Enhanced glycolysis was decreased in TSPO-KO cells by restoring TSPO-GFP expression but not by GFP alone (Fig. 4C and D). Collectively, these findings suggest that TSPO regulates glycolytic metabolism and that TSPO deficiency results in enhanced glycolysis.

Next, we examined the levels of key glycolysis-associated enzymes, including glucose transporter 1 (GLUT1), hexokinase I (HK1), hexokinase II (HK2), pyruvate kinase (PK), and lactate dehydrogenase (LDH), in TSPO-KO GL261 cells and their xenograft tumors. GLUT1, HK2, and LDH levels were significantly increased in TSPO-KO cells (Supplementary Figure 5A and B) and xenograft tumors compared with WT cells and tumors (Fig. 4E and F). Immunohistochemical analysis also showed similar patterns of GLUT1 and HK2 expression in TSPO-KO gliomas and WT gliomas (Fig. 4G–J). However, no significant differences were observed in HK1 and PK expression

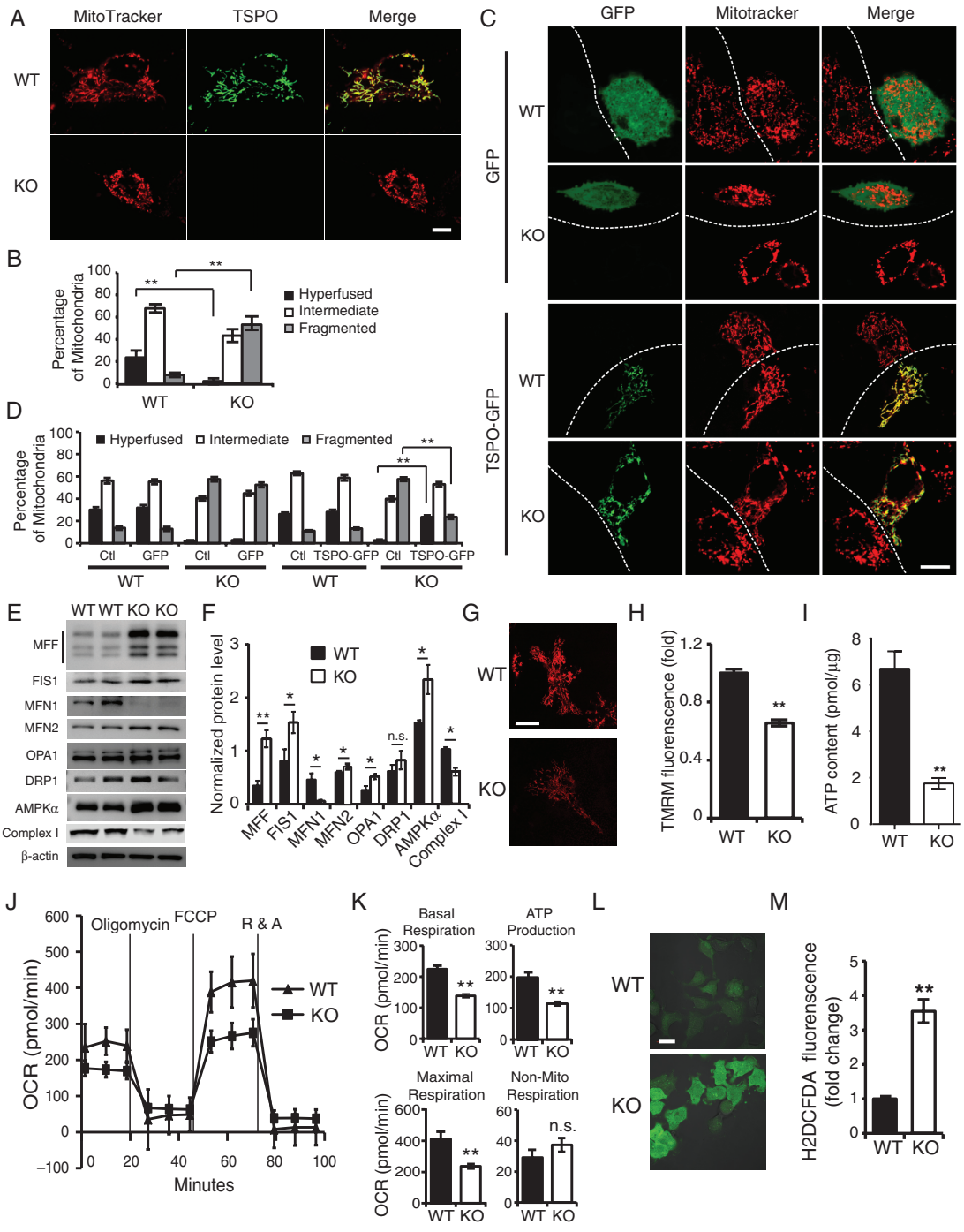

Fig. 3 TSPO deficiency results in a larger number of fragmented mitochondria and a metabolic shift toward glycolysis. (A) Representative images of the mitochondria in KO and WT cells visualized with MitoTracker staining (red). TSPO was stained with an anti-TSPO antibody (green). Scale bar, 10 μm. (B) Quantification of different types of Mito-DsRed2-labeled mitochondria in (A). (C) Representative confocal microscopy images of the mitochondrial morphology in WT and KO cells transfected with TSPO-GFP or GFP expression vectors. Scale bar, 10 μm. (D) Quantification of different types of Mito-DsRed2-labeled mitochondria in (C). (E) Western blot analysis of the levels of mitochondrial fission/fusion proteins in TSPO-KO and WT GL261 cells. (F) Quantification of the western blot results shown in (E). (G and H) Representative images (G) and quantitative analysis (H) of TMRM staining in TSPO-KO and WT GL261 cells. Scale bar, 10 μm. (I) Measurement of ATP levels in TSPO-KO and WT GL261 cells. (J) Mitochondrial stress test to detect mitochondrial energy metabolism and respiratory functions in WT and KO GL261 cells. (K) Quantification of the mitochondrial stress test in (J). (L) Representative images (L) and quantification of ROS production (M) in both TSPO-KO and WT GL261 cells incubated with H2DCFDA. Scale bar, 10 μm. Three independent experiments were performed. The data are presented as means ± SEM. $^{*}P < 0.05$, $^{**}P < 0.01$, and n.s., not significant as determined using Student's *t*-test (B, D, F, H, I, K, and M).

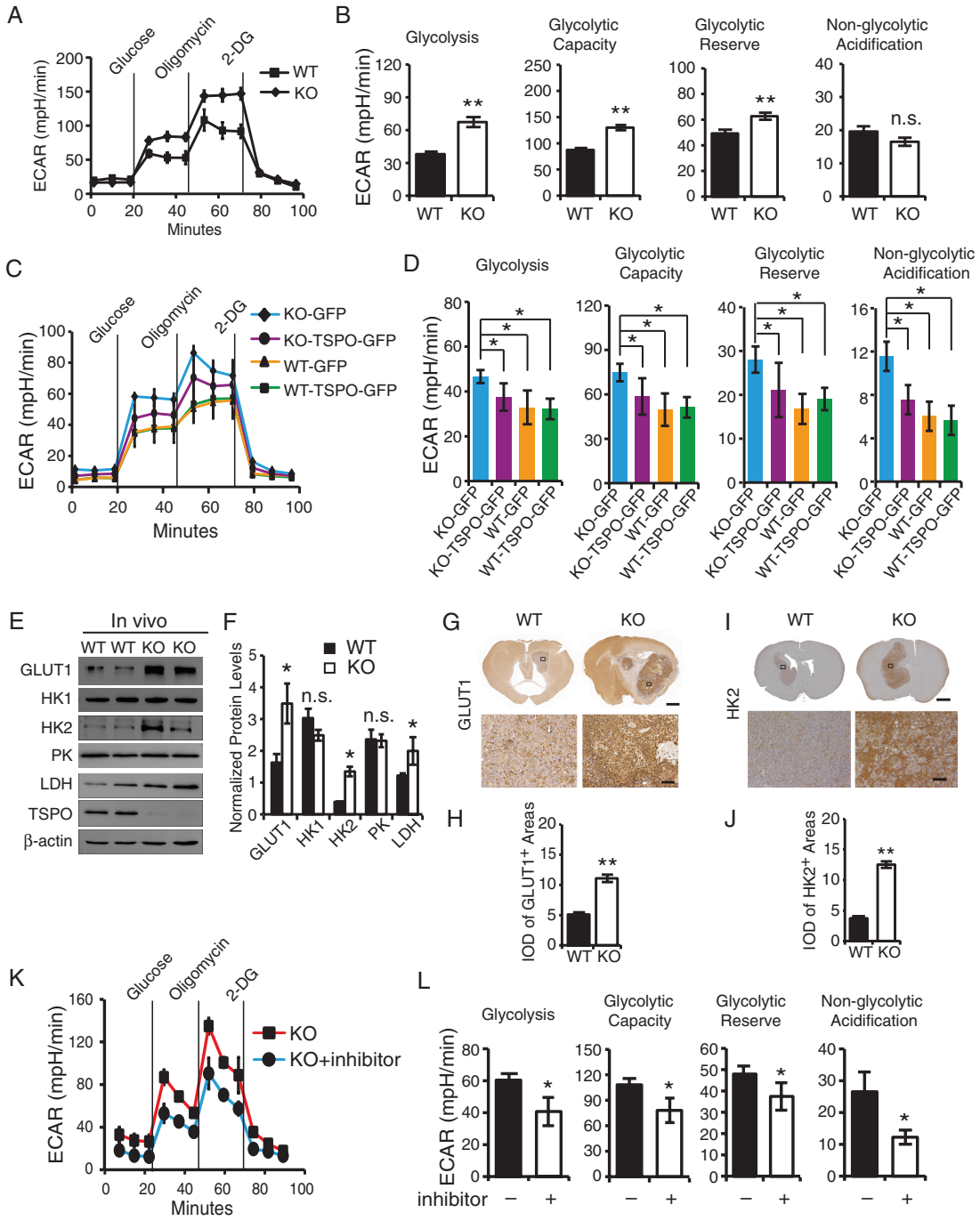

Fig. 4 TSPO deficiency enhances glycolysis in GL261 cells and gliomas. (A) The glycolytic stress test to measure glycolytic activities in TSPO-KO and WT GL261 cells. (B) Quantification of glycolysis, glycolytic capacity, glycolytic reserve and nonglycolytic acidification in (A). (C) Measurement of glycolytic activities in TSPO-KO and WT GL261 cells transfected with TSPO-GFP or GFP expression constructs. (D) Quantification of glycolytic activities in (C). (E) Western blot analysis of the levels of GLUT1, HK1, HK2, PK, and LDH in TSPO-KO and WT gliomas. (F) Normalized levels of the proteins shown in (E). (G) Representative images of immunohistochemical staining with an anti-GLUT1 antibody to examine GLUT1 expression in TSPO-KO and WT gliomas. Scale bar, 1 mm for images in the upper panels and 100 μm for images in the lower panels. (H) Quantification of GLUT1 expression in TSPO-KO or WT gliomas shown in (G). (I) Representative images of immunohistochemical staining with an anti-HK2 antibody to examine HK2 expression in TSPO-KO and WT gliomas. Scale bar, 1 mm for images in the upper panels and 100 μm for images in the lower panels. (J) Quantification of HK2 expression in TSPO-KO and WT gliomas shown in (I). (K) Measurement of glycolytic activities in TSPO-KO GL261 cells treated with the HIF-1α inhibitor PX-478 hydrochloride. (L) Quantification of glycolytic activities in (K). Three independent experiments were performed. The data are presented as means ± SEM. *$P < 0.05$, **$P < 0.01$, and n.s., not significant as determined using Student's *t*-test (B, D, F, H, J, and L).

(Fig. 4E and F, Supplementary Figure 5C and D). Thus, TSPO regulates glycolysis by modulating GLUT1 and HK2 levels. HIF-1α is a crucial factor that regulates glycolysis by inducing the expression of key glycolysis-associated enzymes,[21] and HIF-1α was found to be upregulated in TSPO-KO cells (Fig. 2I and J). Thus, we applied HIF-1α inhibitors to determine whether glycolytic adaptation in TSPO-KO cells depends on the upregulation of HIF-1α. The increased glycolysis observed in TSPO-KO cells was completely blocked by HIF-1α inhibitors (Fig. 4K and L). Collectively, these results suggest that TSPO deficiency triggers HIF-1α upregulation, which likely leads to GLUT1, HK2, and LDH induction and enhanced glycolysis.

TSPO Deficiency Increases Cell Proliferation, Inhibits Mitochondrial Function, and Enhances Glycolysis in Patient-Derived Stemlike GBM1B Cells

We studied the effects of TSPO deficiency on patient-derived stemlike GBM1B cells to determine whether our findings from mouse glioma cells could be replicated in human glioma models. The level of TSPO was decreased by 65% in GBM1B cells transfected with a lentivirus carrying the TSPO short hairpin (sh)RNA (Supplementary Figure 6A). TSPO knockdown significantly increased cell proliferation 24 hours after shRNA transfection (Supplementary Figure 6B). In addition, it significantly inhibited mitochondrial function and increased glycolytic metabolism in GBM1B cells (Supplementary Figure 6C–F). We obtained similar results in human glioma U87MG cells (Supplementary Figure 7). Therefore, our results from mouse GL261, human U87MG, and patient-derived stemlike GBM1B models support the hypothesis that TSPO deficiency promotes glioma growth, and the underlying mechanisms may involve the suppression of mitochondrial function and an increase in glycolysis.

TSPO Deficiency Increases Glucose Uptake and Lactic Acid Conversion

The levels of glucose, lactic acid, and pyruvate in the tumor microenvironment are widely used markers for monitoring dynamic metabolic levels during oxidative phosphorylation and glycolysis.[22,23] We found a significant increase in glucose levels in TSPO-KO cells and tumors compared with WT controls (Fig. 5A and B). When measuring levels of 2-DG6P (2-deoxy-D-glucose-6-phosphate), we observed significantly increased glucose uptake in TSPO-KO cells compared with WT cells (Fig. 5C). We also observed a significant increase in pyruvate levels but a decrease in acetyl CoA levels in TSPO-KO cells compared with WT cells (Fig. 5D and E), indicating that TSPO deficiency causes pyruvate accumulation in TSPO-KO cells.

Next, we measured pyruvate and acetyl CoA levels in isolated mitochondrial and cytosolic fractions from TSPO-KO and WT GL261 cells, and we observed a significant decrease in pyruvate in the mitochondria of TSPO-KO GL261 cells compared with WT GL261 cells. Conversely, pyruvate levels in the cytosol were higher in TSPO-KO cells than in WT cells (Fig. 5F). Furthermore, acetyl CoA levels were reduced in the mitochondria of TSPO-KO cells compared with WT mitochondria (Fig. 5G). Taken together, these findings indicate that TSPO deficiency blocks pyruvate entry into the mitochondria for conversion into acetyl CoA and subsequently results in decreased oxidative phosphorylation and enhanced glycolysis.

We also examined the levels of lactic acid, the final molecule in the glycolytic pathway, in TSPO-KO GL261 cells and xenograft tumors. Lactic acid levels in supernatants from TSPO-KO cells were significantly increased compared with those from WT cells (Fig. 5H). In addition, higher lactic acid levels were observed in both TSPO-KO GL261 cells and xenografts than in WT controls (Fig. 5I and J), which was also confirmed by the results of a metabolic flux assay using [U-$^{13}C_6$] glucose tracing (Supplementary Figure 8). Overall, our results support the hypothesis that a TSPO deficiency in glioma cells affects mitochondrial function and shifts the metabolic pathway toward glycolysis.

A TSPO Antagonist Promotes Glioma Growth by Inducing a Metabolic Shift Toward Glycolysis

Finally, we investigated the effects of the TSPO antagonist PK11195 and agonist Ro5-4864 on glioma growth using a mouse GL261 xenograft glioma model. We observed a significantly greater average tumor volume in the PK11195 group than in the phosphate buffered saline (PBS) control and Ro5-4864 groups (Fig. 6A and B). However, the TSPO agonist Ro5-4864 did not produce a significant difference compared with the PBS group. Importantly, HE staining also indicated that PK11195-mediated inhibition caused robust hemorrhaging and more abundant blood vessels in gliomas compared with those in the PBS or Ro5-4864 groups (Fig. 6B). Taken together, TSPO inhibition also promotes glioma growth and malignancy.

Next, we measured the effects of PK11195 and Ro5-4864 on the glycolytic and mitochondrial oxidative phosphorylation capacities of GL261 cells. The inhibition of TSPO with PK11195 significantly increased glycolysis (Fig. 6C and D) and decreased mitochondrial function (Fig. 6E and F). Intriguingly, activation of TSPO with Ro5-4864 also significantly decreased mitochondrial function (Fig. 6E and F), although no obvious effect on the glycolytic capacity of GL261 cells was observed (Fig. 6C and D). Together, our results support the hypothesis that TSPO deficiency or inhibition promotes glioma growth and angiogenesis by inducing a metabolic shift toward glycolysis.

Discussion

TSPO is highly expressed in many types of cancer. However, the role of TSPO in regulating tumor development remains controversial. Herein, by applying the "loss of function" strategy we demonstrated that TSPO KO promotes glioma cell proliferation and glioma growth, and the underlying molecular mechanism is likely involved in mitochondrial dysfunction and glycolysis enhancement. A dynamic balance between oxidative phosphorylation and glycolysis is

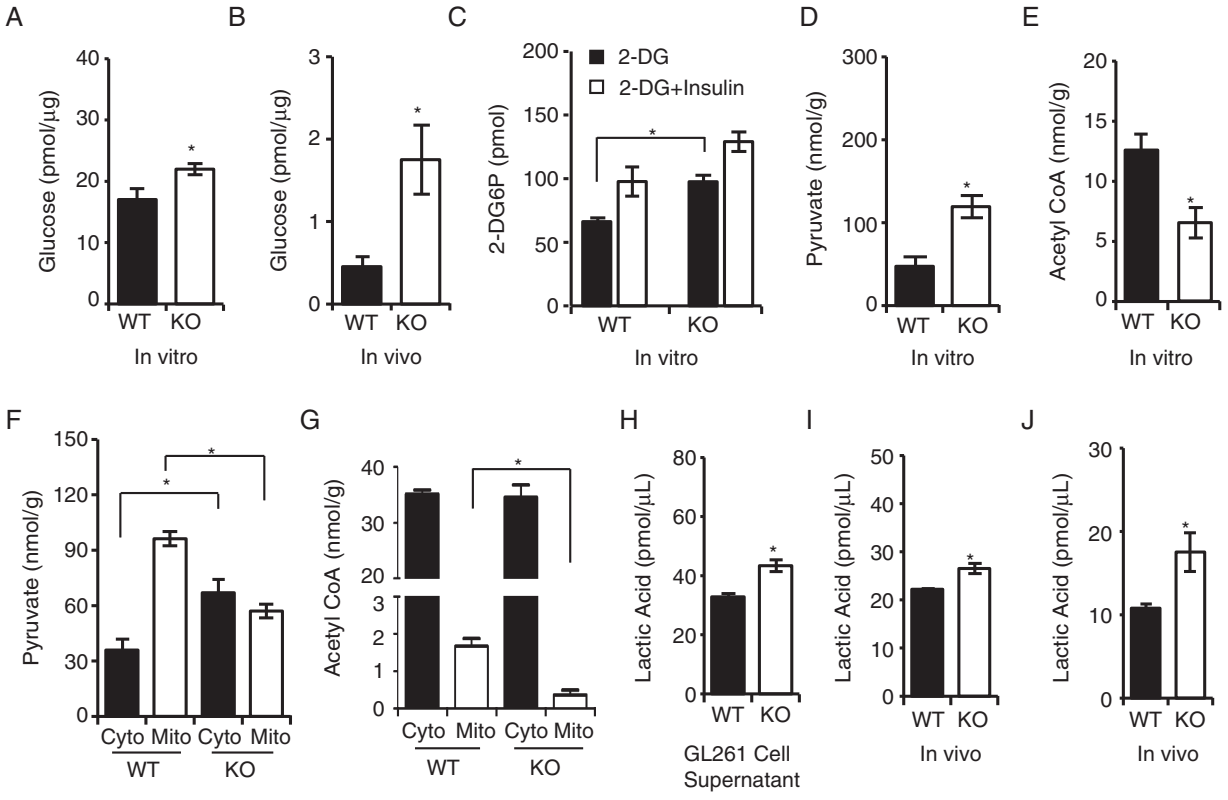

Fig. 5 TSPO regulates glucose uptake and lactic acid conversion. (A and B) Glucose fluorometric assay to measure glucose levels in GL261 cells (in vitro) (A) and gliomas (in vivo) (B). (C) Glucose uptake assay to examine glucose uptake capacities in TSPO-KO and WT cells. Insulin stimulation was used as a positive control. (D) Colorimetric assay to measure pyruvate levels in TSPO-KO and WT GL261 cells. (E) Fluorometric assay to detect acetyl CoA levels in TSPO-KO and WT GL261 cells. (F) Colorimetric assay to measure pyruvate levels in the isolated mitochondria and cytosol from TSPO-KO and WT GL261 cells. (G) Fluorometric assay to measure acetyl CoA levels in isolated mitochondria and cytosol from TSPO-KO and WT GL261 cells. (H–J) Fluorometric assay to measure lactic acid levels in cell culture supernatants (H), GL261 cells (I), and gliomas (J). Three independent experiments were performed. The data are presented as means ± SEM. $^{*}P < 0.05$ and $^{**}P < 0.01$ as determined using Student's *t*-test (A, B, C, D, E, F, G, H, I, and J).

essential for cell survival in response to changes in metabolism. While normal resting cells typically rely on mitochondrial oxidative phosphorylation to meet bioenergetic needs, tumor cells often utilize glycolysis to provide the energy and carbon needed to meet the high metabolic demands of tumor growth and survival.[20] In this study, we observed a morphological change in mitochondria in TSPO-KO GL261 cells. TSPO deficiency caused mitochondrial fragmentation and decreased ATP production and mitochondrial oxidative phosphorylation. However, the glycolytic capacity was enhanced, possibly representing a major contribution to the increased proliferative activity of TSPO-KO GL261 cells. We also focused on investigating the effects of TSPO deletion on the glucose metabolism pathway. The expression levels of the glycolysis trigger HIF-1α, and several key glycolytic enzymes (eg, GLUT1, HK2, LDH) were significantly elevated in TSPO-KO GL261 cells and glioma xenografts, resulting in increased glucose uptake and lactic acid conversion. Thus, the increased proliferation and tumorigenicity of TSPO-KO cells are likely due to a metabolic shift toward glycolysis, wherein the "Warburg effect" is enhanced to facilitate the malignancy of TSPO-KO cells.[20,23] Our data support previous findings that the use of glycolysis versus mitochondrial respiration depends on the specific microenvironment in GBM.[24]

In addition to tumor cell–intrinsic changes, TSPO deficiency also increased angiogenesis, one of the typical features of malignant tumors. Pro-angiogenic factors including various forms of VEGF-A, MMP, and IL-8 participate in triggering the development of the vascular network.[25,26] In our study, the levels of HIF-1α, VEGF-A, MMP2, and IL-8, which are key factors regulating angiogenesis in tumor tissues, were increased in glioma tissues when TSPO expression was completely silenced. These results support the hypothesis that TSPO deficiency in glioma establishes a tumor-promoting microenvironment through hypoxia-induced angiogenesis and a metabolic shift toward glycolysis.

TSPO expression is highly upregulated in various tumor types, such as breast, colorectal, and prostate cancers as well as glioma. Previous studies reported that TSPO expression in human astrocytoma was correlated with the grade of malignancy, proliferation, apoptosis, and survival,[8,15]

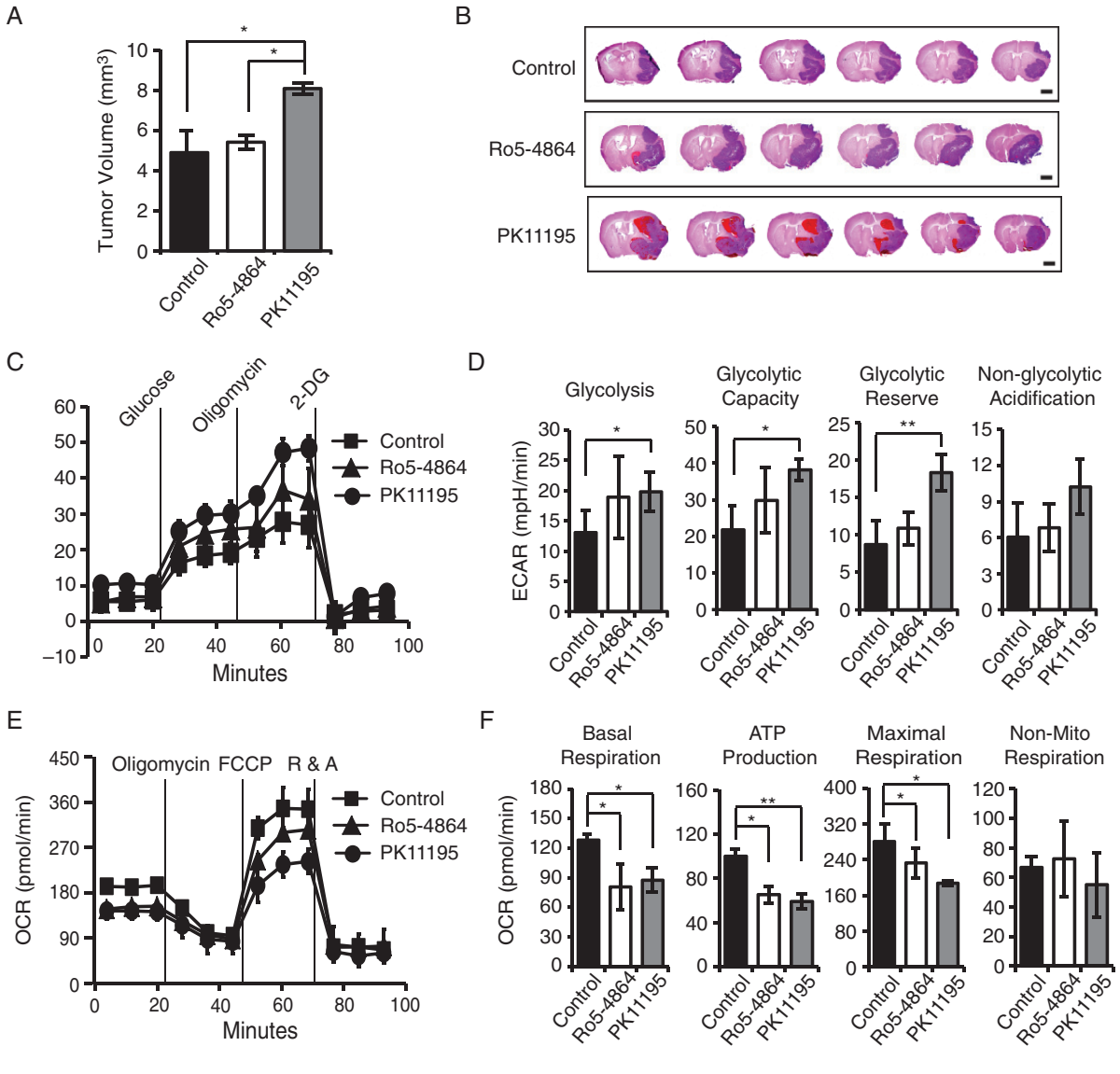

Fig. 6 A TSPO antagonist promotes glioma growth by suppressing mitochondrial energy metabolism and increasing glycolysis. (A) Quantification of tumor volumes from mice 30 days after the intracranial injection of WT GL261 cells and treatment with PK11195, Ro5-4864, or PBS. PBS served as the control. (B) Representative images of HE staining in a series of slices from the brains of mice treated with PK11195, Ro5-4864, or PBS. Scale bar, 2 mm. (C) Measurement of glycolytic activities in GL261 cells treated with different compounds. (D) Quantification of glycolytic activities in (C). (E) Mitochondrial stress test to detect mitochondrial energy metabolism and respiratory functions in GL261 cells treated with different compounds. (F) Quantification of the mitochondrial stress test in panel (E). The data are presented as means ± SEM. *$P < 0.05$ and **$P < 0.01$ as determined using Student's *t*-test (A, D, and F).

suggesting that TSPO promotes astrocytoma growth and could be a biomarker for evaluating malignancy or a target for developing anti-astrocytoma approaches. However, immunochemical staining showed only a small number of TSPO-positive cells (16.7 ± 6.4%) in astrocytoma samples,[8] indicating that many astrocytoma cells displayed a relatively low TSPO expression. In fact, in some tumors of the adrenals, skin, and liver, the levels of TSPO generally decreased compared with those of their normal tissues.[27] These findings demonstrated that elevated TSPO expression is not a common feature of aggressive tumors. TSPO expression is also highly upregulated in many inflammatory diseases, including Alzheimer's disease and Parkinson's disease.[28,29] Increasing evidence has revealed that the upregulation of TSPO expression is related to the inflammatory microenvironment and can be induced by inflammatory signaling pathways as described previously.[30,31]

Our results also showed high TSPO expression in GBM samples. However, our findings clearly demonstrate a significant role for TSPO in regulating the dynamic balance between oxidative phosphorylation and glycolysis and that

TSPO is essential for cellular and mitochondrial metabolism, which is also supported by a recent study.[32] Accordingly, our findings strongly suggest that TSPO may not constitute a good biomarker for evaluating the malignancy or a target for developing prospective approaches against GBM. Regardless, additional studies, especially conditional TSPO transgenic mouse models, are necessary to establish a more precise correlation between TSPO expression levels and tumor malignancy and to more clearly understand the dynamic functions of TSPO during tumorigenesis.

In summary, this study elucidated novel biological functions for TSPO in regulating glioma growth, angiogenesis, and metabolism. TSPO deficiency or inhibition promotes glioma growth by suppressing mitochondrial function and increasing glycolysis and hypoxia-induced angiogenesis. This study establishes a new foundation for exploring aspects of TSPO biology and provides a better understanding of TSPO-regulated molecular mechanisms, including the regulation of mitochondrial functions, glycolysis, and angiogenesis.

Supplementary Material

Supplementary data are available at *Neuro-Oncology* online.

Keywords

angiogenesis | glioma | glycolysis | mitochondrial oxidative phosphorylation |TSPO

Funding

This work was supported by the National Natural Science Foundation of China (31471016, 91542117, 81673010, 81471574, and 81602503), the CAMS Initiative for Innovative Medicine (2016-I2M-1-008), the National Key Research and Development Program of China (2016YFA0101001, 2016YFC0903900), the National Basic Research Program of China (2013CB530503), CAMS Basic Research Expenses (2018PT31052), and the Peking Union Medical College Scholarship for Young Scientists (3332015109).

Acknowledgments

We thank the Guidon Pharmaceutics Platform for assisting with the experiments.

Authorship statement. Y.F. performed experiments, analyzed data, and wrote the manuscript. D.W., C.L., and X.Z. performed animal and cell culture. H.W. and M.C. performed the immunohistochemistry and immunofluorescence staining. Y.H. and H.C. performed flow cytometry. X.Z. assisted with the experimental design of this study. J.Z. and W.H. designed the scheme of the study and edited the manuscript.

Conflict of interest statement. The authors have no potential conflicts of interest to declare.

References

1. Li F, Liu J, Garavito RM, Ferguson-Miller S. Evolving understanding of translocator protein 18 kDa (TSPO). *Pharmacol Res.* 2015;99:404–409.
2. Lacapère JJ, Papadopoulos V. Peripheral-type benzodiazepine receptor: structure and function of a cholesterol-binding protein in steroid and bile acid biosynthesis. *Steroids.* 2003;68(7–8):569–585.
3. Banati RB, Middleton RJ, Chan R, et al. Positron emission tomography and functional characterization of a complete PBR/TSPO knockout. *Nat Commun.* 2014;5:5452.
4. Wang H, Zhai K, Xue Y, et al. Global deletion of TSPO does not affect the viability and gene expression profile. *PLoS One.* 2016;11(12):e0167307.
5. Kelly-Hershkovitz E, Weizman R, Spanier I, et al. Effects of peripheral-type benzodiazepine receptor antisense knockout on MA-10 Leydig cell proliferation and steroidogenesis. *J Biol Chem.* 1998;273(10):5478–5483.
6. Liu GJ, Middleton RJ, Hatty CR, et al. The 18 kDa translocator protein, microglia and neuroinflammation. *Brain Pathol.* 2014;24(6):631–653.
7. Maaser K, Grabowski P, Oezdem Y, et al. Up-regulation of the peripheral benzodiazepine receptor during human colorectal carcinogenesis and tumor spread. *Clin Cancer Res.* 2005;11(5):1751–1756.
8. Vlodavsky E, Soustiel JF. Immunohistochemical expression of peripheral benzodiazepine receptors in human astrocytomas and its correlation with grade of malignancy, proliferation, apoptosis and survival. *J Neurooncol.* 2007;81(1):1–7.
9. Wen PY, Kesari S. Malignant gliomas in adults. *N Engl J Med.* 2008;359(5):492–507.
10. Su Z, Roncaroli F, Durrenberger PF, et al. The 18-kDa mitochondrial translocator protein in human gliomas: an 11C-(R)PK11195 PET imaging and neuropathology study. *J Nucl Med.* 2015;56(4):512–517.
11. Su Z, Herholz K, Gerhard A, et al. [^{11}C]-(R)PK11195 tracer kinetics in the brain of glioma patients and a comparison of two referencing approaches. *Eur J Nucl Med Mol Imaging.* 2013;40(9):1406–1419.
12. Teplyuk NM, Uhlmann EJ, Gabriely G, et al. Therapeutic potential of targeting microRNA-10b in established intracranial glioblastoma: first steps toward the clinic. *EMBO Mol Med.* 2016;8(3):268–287.
13. Lim JA, Li L, Kakhlon O, Myerowitz R, Raben N. Defects in calcium homeostasis and mitochondria can be reversed in Pompe disease. *Autophagy.* 2015;11(2):385–402.
14. Figarola JL, Singhal J, Tompkins JD, et al. SR4 uncouples mitochondrial oxidative phosphorylation, modulates AMP-dependent kinase (AMPK)-mammalian target of rapamycin (mTOR) signaling, and inhibits proliferation of HepG2 hepatocarcinoma cells. *J Biol Chem.* 2015;290(51):30321–30341.
15. Miettinen H, Kononen J, Haapasalo H, et al. Expression of peripheral-type benzodiazepine receptor and diazepam binding inhibitor in human astrocytomas: relationship to cell proliferation. *Cancer Res.* 1995;55(12):2691–2695.
16. Weiss WA, Burns MJ, Hackett C, et al. Genetic determinants of malignancy in a mouse model for oligodendroglioma. *Cancer Res.* 2003;63(7):1589–1595.
17. Hiraga T. Hypoxic microenvironment and metastatic bone disease. *Int J Mol Sci.* 2018;19(11):1–15.
18. Moreira PI, Carvalho C, Zhu X, Smith MA, Perry G. Mitochondrial dysfunction is a trigger of Alzheimer's disease pathophysiology. *Biochim Biophys Acta.* 2010;1802(1):2–10.

19. Oparka M, Walczak J, Malinska D, et al. Quantifying ROS levels using CM-H2DCFDA and HyPer. *Methods*. 2016;109:3–11.
20. Potter M, Newport E, Morten KJ. The Warburg effect: 80 years on. *Biochem Soc Trans*. 2016;44(5):1499–1505.
21. Ajduković J. HIF-1—a big chapter in the cancer tale. *Exp Oncol*. 2016;38(1):9–12.
22. Olson KA, Schell JC, Rutter J. Pyruvate and metabolic flexibility: illuminating a path toward selective cancer therapies. *Trends Biochem Sci*. 2016;41(3):219–230.
23. San-Millán I, Brooks GA. Reexamining cancer metabolism: lactate production for carcinogenesis could be the purpose and explanation of the Warburg effect. *Carcinogenesis*. 2017;38(2): 119–133.
24. Talasila KM, Røsland GV, Hagland HR, et al. The angiogenic switch leads to a metabolic shift in human glioblastoma. *Neuro Oncol*. 2017;19(3):383–393.
25. Zarogoulidis P, Katsikogianni F, Tsiouda T, Sakkas A, Katsikogiannis N, Zarogoulidis K. Interleukin-8 and interleukin-17 for cancer. *Cancer Invest*. 2014;32(5):197–205.
26. Mahecha AM, Wang H. The influence of vascular endothelial growth factor-A and matrix metalloproteinase-2 and -9 in angiogenesis, metastasis, and prognosis of endometrial cancer. *Onco Targets Ther*. 2017;10:4617–4624.
27. Han Z, Slack RS, Li W, Papadopoulos V. Expression of peripheral benzodiazepine receptor (PBR) in human tumors: relationship to breast, colorectal, and prostate tumor progression. *J Recept Signal Transduct Res*. 2003;23(2–3):225–238.
28. Ghadery C, Koshimori Y, Christopher L, et al. The interaction between neuroinflammation and beta-amyloid in cognitive decline in Parkinson's disease. *Mol Neurobiol*. 2019. doi: 10.1007/s12035-019-01714-6.
29. Gui Y, Marks JD, Das S, Hyman BT, Serrano-Pozo A. Characterization of the 18 kDa translocator protein (TSPO) expression in post-mortem normal and Alzheimer's disease brains. *Brain Pathol*. 2019. doi: 10.1111/bpa.12763.
30. Zinnhardt B, Pigeon H, Thézé B, et al. Combined PET imaging of the inflammatory tumor microenvironment identifies margins of unique radiotracer uptake. *Cancer Res*. 2017;77(8):1831–1841.
31. Werry EL, Bright FM, Piguet O, et al. Recent developments in TSPO PET imaging as a biomarker of neuroinflammation in neurodegenerative disorders. *Int J Mol Sci*. 2019;20(13):1–21.
32. Milenkovic VM, Slim D, Bader S, et al. CRISPR-Cas9 mediated TSPO gene knockout alters respiration and cellular metabolism in human primary microglia cells. *Int J Mol Sci*. 2019;20(13):1–15.